

Photocatalytic Degradation of Rhodamine B Dye by Bi₂MoO₆ Microspheres under Natural Sunlight Irradiation

¹Gajendra Kumar*, and ²Alok Kumar Gehlot

Author Affiliations

¹Department of Chemistry, Constituent Government College (MJPRU), Hasanpur, Amroha, Uttar Pradesh 244241, India

²Department of Mathematics, Faculty of Engineering, Teerthanker Mahaveer University, Moradabad, Uttar Pradesh 244001, India

*Corresponding Author

Gajendra Kumar, Department of Chemistry, Constituent Government College (MJPRU), Hasanpur, Amroha, Uttar Pradesh 244241, India
E-mail: gaj.chem@gmail.com, gandhravk.engineering@tmu.ac.in

Received on 27.11.2022, Revised on 18.01.2023, Approved on 07.05.2023, Accepted on 15.03.2023, Published on 20.06.2023

ABSTRACT

Removal of dyes from water bodies is a significant concern throughout the world. In this study, Bi₂MoO₆ microspheres were synthesized by a hydrothermal synthetic route at 180°C, and it is effectively characterized by various techniques. The XRD peaks confirmed the orthorhombic planes of Bi₂MoO₆. The microsphere-like morphology was revealed by FESEM and HRTEM. The optical band gap was investigated by UV-vis DRS and showed a reflection edge with corresponding energy at 2.68 eV. The photocatalytic activity of the Bi₂MoO₆ microsphere is tested against the degradation of rhodamine B under natural sunlight irradiation. About 90% degradation of rhodamine B is observed in 90 min with the photocatalytic degradation rate of 0.038min⁻¹. Results confirmed that the Bi₂MoO₆microspherecould facilitate 90% degradation of RhB dye and followed the first-order kinetic model.

Keywords: Bi₂MoO₆; Solar Photocatalyst; Rhodamine B, Photocatalysis

How to cite this article: Kumar G. and Gehlot A.K. (2023). Photocatalytic Degradation of Rhodamine B Dye by Bi₂MoO₆ Microspheres under Natural Sunlight Irradiation. *Bulletin of Pure and Applied Sciences-Chemistry*, 42C (1), 1-8.

INTRODUCTION

Organic dyes in aquatic environments are a significant pollutant due to their extensive usage in textile and other fabric industries (Homem & Santos, 2011; Qin et al., 2021; Rivera-Utrilla et al., 2013). Many water sources are polluted by residual dyes, which enter directly into the aquatic environment through various means like dye industries, textile industries, etc. (Dinh et al., 2017; Michael et al., 2013). Rhodamine B dye is a widely used cationic dye found in its application in coloring fabrics. Rhodamine B is water-

soluble, stable in an aquatic environment, non-biodegradable, and cancer-causing in nature, which makes it harmful to humans and living species of aquatic ecosystems.

However, these residual dyes are not quickly metabolized, so they can easily pollute groundwater and surface water, causing harmful diseases in animals and humans. Due to this, several methods have been developed for wastewater remediation. Out of these techniques, semiconductor-based photocatalysts are widely utilized for the photocatalytic

removal of various water pollutants (Akbari et al., 2021; Calvete et al., 2019; Durán-Álvarez et al., 2016). To date, ZnO and TiO_2 nanoparticles are the most commonly used photocatalysts for degrading organic dyes, but they require UV light for photoexcitation as their band gap is large. Recently, bismuth-based photocatalysts have been the most promising and new class of photocatalysts used in wastewater treatment over the last few decades. Their applications cover several areas such as water-splitting, NH_3 production from N_2 , reduction of CO_2 , and degradation of water pollutants through heterogeneous photocatalysis. The band structure of these materials provides them with a suitable band gap for visible light-active and a well-distributed valence band in favor of recombination charge, enabling them to act as potential photocatalytic materials for wastewater treatment over metal oxides. Bismuth-based multi-component oxides are usually identified as stoichiometric hybrid oxides of Bi_2O_3 and metal oxides like TiO_2 , V_2O_5 , Mo_2O_3 , W_2O_3 , etc. The Aurivillius layered structure is generally determined by $[\text{Bi}_2\text{O}_2]^{2+}$ layers combined with metal oxide layers along the c-axis. The Bi_2MoO_6 ($n = 1$) is the simplest member of the Aurivillius family, which is a promising candidate for the photocatalytic degradation of inorganic and organic pollutants, under solar-light illumination. In this work, we have reported the synthesis of Bi_2MoO_6 microsphere as a solar photocatalyst, and its photocatalytic activity was tested on RhB dye degradation under solar light irradiation.

Synthesis of Bi_2MoO_6 microsphere

4 mmol bismuth nitrate pentahydrate was mixed in 20 mL of ethylene glycol, and 4 mmol sodium molybdate dihydrate was dissolved in 30 mL of ethyl alcohol. After stirring both the solutions for 30 min separately, the sodium molybdate dihydrate solution was added slowly into the bismuth nitrate pentahydrate solution with continuous magnetic stirring. After 45 min

of constant stirring, the mixture was poured into a Teflon-lined stainless-steel autoclave and heated under a controlled temperature of 180°C for 24 h. The finally prepared precipitates were washed with DI water and $\text{C}_2\text{H}_5\text{OH}$ and separated by centrifugation at 10000 RPM for 20 min, and the white product finally obtained was dried in an oven at 50°C .

Methodology for Photocatalytic Experiment

The photocatalytic performance of the Bi_2MoO_6 photocatalyst was determined by observing the degradation of RhB dye (10 mg/L) solutions under exposure to natural sunlight radiation. Typically, 100 mL aqueous solution of 10 ppm RhB dye is taken into a 500 mL beaker, followed by the addition of 80 mg of Bi_2MoO_6 photocatalysts into it, which was then subjected to continuous stirring for 60 min under the dark condition. After 60 min of dark study, the beaker was kept under sunlight. 2 mL aliquot was taken from the beaker at certain intervals. The change in concentration of the RhB molecule was recorded by UV-vis spectrophotometer (UV-1800, Shimadzu, Japan) at absorbance $\lambda = 553$ nm.

RESULTS AND DISCUSSIONS

Characterization of Bi_2MoO_6

XRD analysis

The XRD spectra of pristine Bi_2MoO_6 was investigated by Bruker AXS advanced diffractometer with a scan range of 1 min^{-1} using graphite monochromatized $\text{Cu K}\alpha$ radiation (1.5418 \AA) operated at 40 kilovolts. The XRD peaks for Bi_2MoO_6 were detected at $2\theta = 11.1^\circ, 28.5^\circ, 32.9^\circ, 36.2^\circ, 47.2^\circ, 55.6^\circ, 58.4^\circ$, which are matched to (020), (131), (002), (151), (062), (133), and (262) orthorhombic planes of Bi_2MoO_6 (JCPDS Card No.- 21 1272) (Figure.1). The lattice parameters are calculated to be as $a = 5.42 \text{ \AA}$, $b = 16.32 \text{ \AA}$, and $c = 5.42 \text{ \AA}$, with the average crystallite size of 14.10 nm.

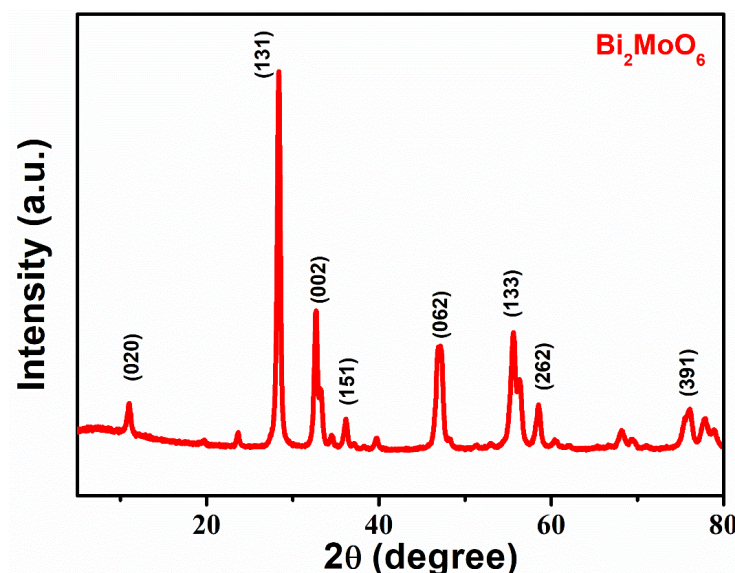


Figure 1: XRD patterns of as-synthesized Bi_2MoO_6 microspheres

Morphology of Bi_2MoO_6

The surface morphology of the Bi_2MoO_6 photocatalyst was investigated by electron microscopy. The FE-SEM image of Bi_2MoO_6 microspheres was recorded by Zeiss FESEM, Ultra-plus 55 shows agglomeration of nanospikes-like structures (Figure. 2a and 2b).

Similarly, the morphology of the Bi_2MoO_6 microsphere was better displayed from the HRTEM images with their corresponding SAED pattern (Figure. 2c and 2d) are recorded on a JEM-3200FS, JEOL transmission electron microscope.

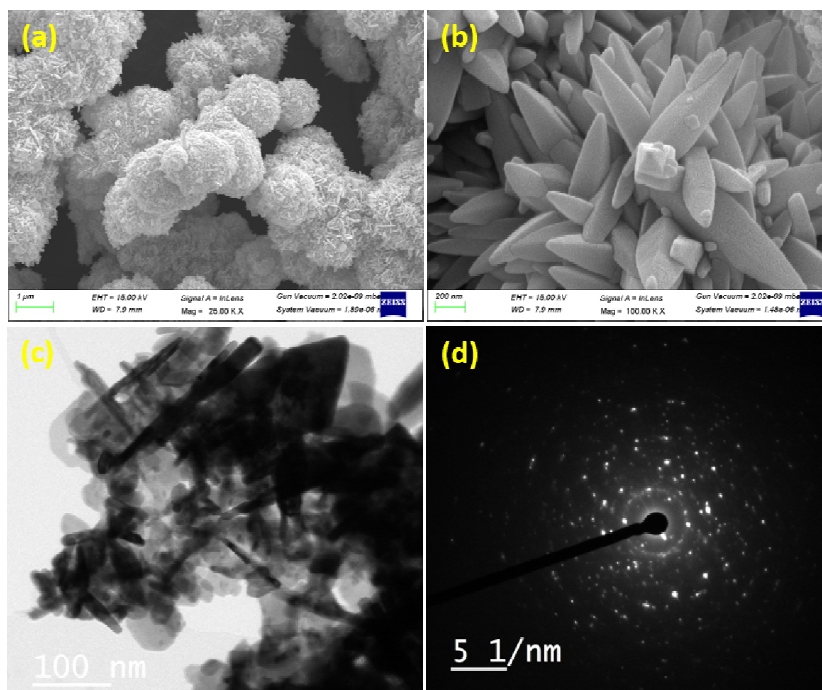


Figure 2: a) FE-SEM image of Bi_2MoO_6 microspheres; b) HR-TEM image of Bi_2MoO_6 microspheres

UV-vis DRS analysis

The UV-vis DRS studies of the as-prepared Bi_2MoO_6 microspheres were recorded on a Shimadzu UV-2450, Japan spectrophotometer using BaSO_4 as reference. The pure Bi_2MoO_6 microspheres absorb in the ultraviolet and visible light region (Figure 3). The UV-vis DRS spectra were changed into absorption spectra by using (K-M function) Kubelka-Munk (Kortüm,

1969), and the band gap was calculated from the Taucs plots (Tauc et al., 1966), Figure 3 shows Tauc's plots of Bi_2MoO_6 photocatalyst. The optical band gap of Bi_2MoO_6 was determined to be 2.68 eV.

$$(ah\nu)^{1/n} = A(h\nu - E_g) \quad (1)$$

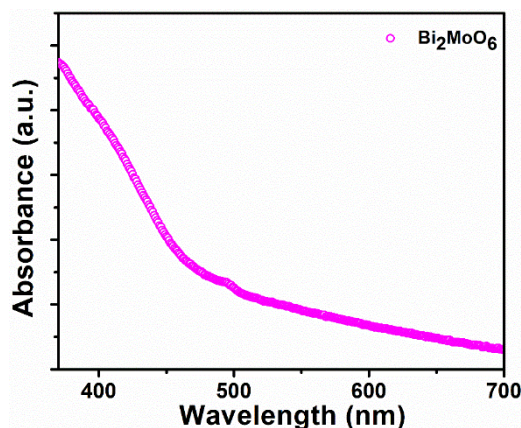


Figure 3: Tauc's plot of pure Bi_2MoO_6

Photocatalytic activity

The impact of photocatalyst dose on the photocatalytic performance was investigated by treating the aqueous solution RhB with different amounts of photocatalyst, i.e., 50–100 mg of photocatalyst per 100mL under the same experimental environment as mentioned above. The degradation rate and removal efficiency were first increased with the increase in the photocatalyst dose from 50 mg ($k=0.08 \text{ min}^{-1}$) to 80 mg/100mL ($k=0.038 \text{ min}^{-1}$) and then decreased for the dose 100 mg ($k=0.011 \text{ min}^{-1}$) (Figure.4a and 4b). The impact of the change in concentration of RhB solution has been investigated by changing the initial concentration of RhB solution from 10 to 30 mg/L. The decrease in the photocatalytic performance was observed with the increase of RhB concentrations (Figures. 4c and 4d). A complete photocatalytic degradation study was performed with a photocatalyst dose of 80 mg per 100 mL aqueous solution of RhB.

The sunlight-mediated photocatalytic degradation of RhB dye (10 mg/L) by the

Bi_2MoO_6 microsphere is shown as a curve of C_t/C_0 vs. (t) time (Figure 4). In the dark experiment firstly, the change in concentration of RhB dye was determined by the dark experiment. About 16% of RhB dye was adsorbed on Bi_2MoO_6 microspheres (Figure 4a). The self-decomposition investigation of rhodamine B shows negligible results. The Bi_2MoO_6 microspheres show the photocatalytic performance of about 90 % rhodamine B dye degradation after 90 min of sunlight exposure. The degradation kinetics of rhodamine B was modelled by a 1st-order kinetics model. The 1storder kinetics equation is:

$$\ln(C_0/C_t) = kt \quad (2)$$

Where C_0 is the initial dye concentration of dye, and C_t is the dye concentration at any time, whereas k (min^{-1}) (Table 1) is the 1st-order kinetic rate constant for RhB dye photocatalytic degradation. The photocatalytic rate constant of pristine Bi_2MoO_6 ($k= 0.038 \text{ min}^{-1}$) (Figure 4b). Figure 4c shows the UV-vis absorption spectra, which shows the change in concentration of

Photocatalytic Degradation of Rhodamine B Dye by Bi₂MoO₆ Microspheres under Natural Sunlight Irradiation

rhodamine B dye during the photocatalytic degradation. The decrease in the intensity of the absorption peak of rhodamine B dye (553 nm)

was observed over 90 min period of sunlight irradiation.

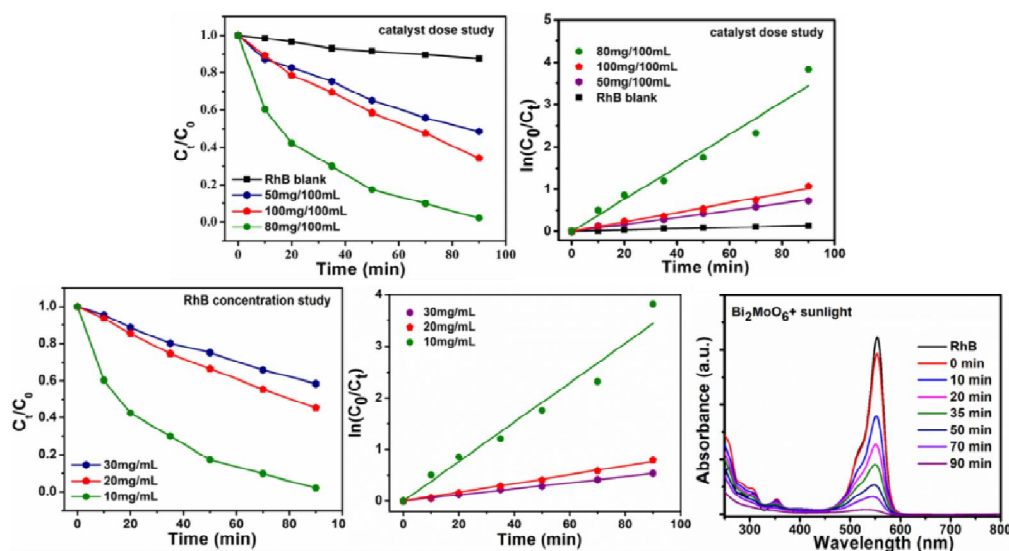


Figure 4: a) Effect of photocatalyst dose on the photocatalytic performance, (b) Corresponding 1storder kinetics curves, (c) Effect of RhB dye concentration on the photocatalytic performance, (d) Corresponding 1storder kinetic curves, (e) UV-vis absorbance spectra of RhB dye solution.

Table1: Summary of kinetics study of RhB dye photocatalytic degradation

Sample name	Percentage Adsorption	Percentage Degradation	1 st -order kinetics (RhB)	
			k (Min ⁻¹)	R ²
Bi ₂ MoO ₆	16%	90%	0.038	0.994
Blank	NA	10%	0.002	0.983

Reusability of photocatalyst

The reusability of the Bi₂MoO₆ photocatalyst has been tested for three successive cycles for the photocatalytic degradation of RhB dye. A similar type of degradation pattern and degradation rate for all three-cycle obtained

(Figure 5a). The chemical stability of Bi₂MoO₆ photocatalyst further confirmed from the XRD pattern and FESEM image of the used photocatalyst obtained after the 3rd cycle (Figure 5b and 5c).

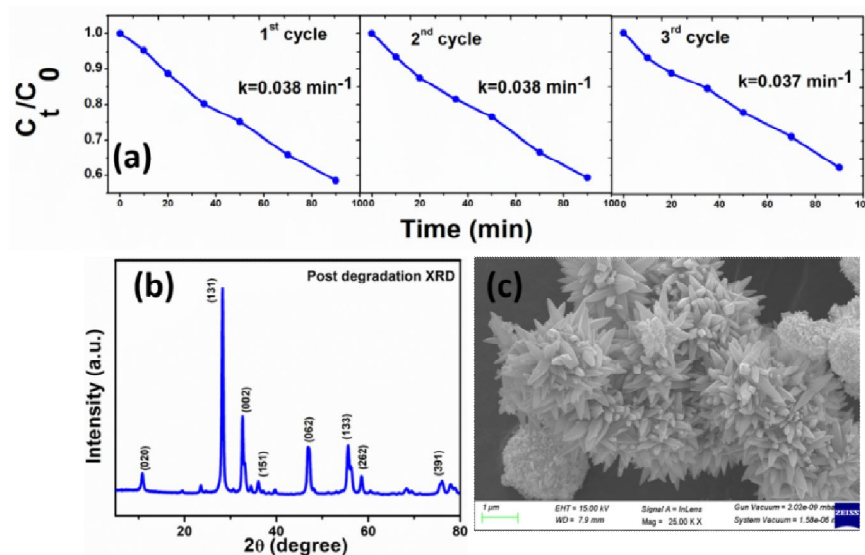


Figure 5: (a) Reusability of the Bi₂MoO₆ up to three cycles; (b) post degradation XRD and (c) SEM image of the re-used photocatalyst.

Reactive oxygen species (ROS) scavenging studies

In order to determine the main active reactive oxygen species responsible for the photocatalytic degradation of RhB, the ROS experiment was performed in the presence of (1mM) ammonium oxalate (h^+), (1mM)

chloroform ($O_2^{\cdot-}$ scavenger) and (1mM) isopropyl alcohol (OH^{\cdot} scavenger) respectively, under the optimized conditions. The radical scavenging experiment confirmed that the $O_2^{\cdot-}$ radical is mainly responsible for the photocatalytic degradation of RhB (Figure 6).

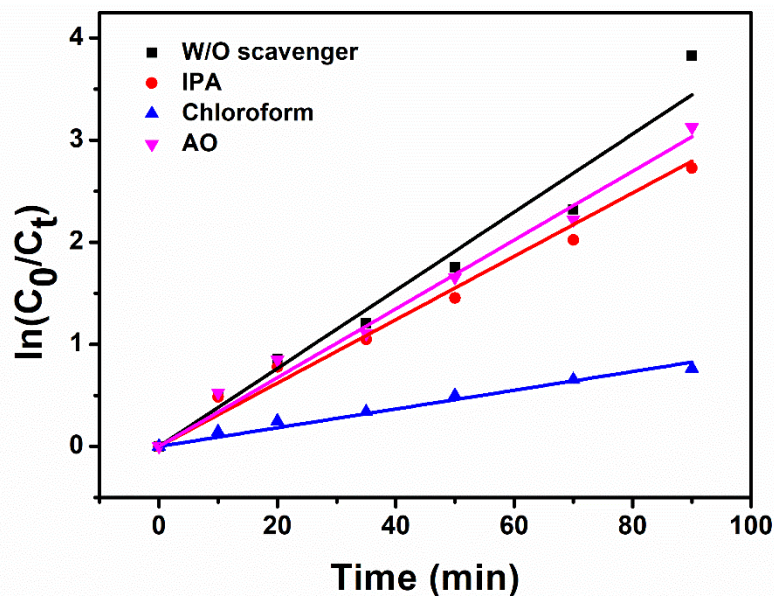


Figure 6: Effect of reactive oxygen species on RhB degradation

Photocatalytic mechanism

The charge transfer in a semiconductor photocatalyst mainly depends on the photocatalysts conduction and valence band

positions. The value of the conduction and valence band is calculated by the equation, $ECB = \chi (AaBb) - 1/2E_g + E_o$ and $EVB = ECB + E_g$ where E_g represents the band gap of

Bi₂MoO₆, ECB represents the conduction band potential, EVB represents the potential of the valence band, and E_o value is taken as - 4.50 eV, i.e., the energy of free electrons on the NHE scale. The value χ (AaBb) represents the absolute electronegativity of a semiconductor material of the AaBb type. For Bi₂MoO₆, the electronegativity value is calculated to be 5.55 eV. Upon exposure to visible light radiation, the electron excited from the valence band into the conduction band. The conduction and valence bands of Bi₂MoO₆ are calculated as -0.28 eV and

+2.40 eV, respectively. The valence band of Bi₂MoO₆ was estimated to be +2.38 eV (vs. NHE), which was more negative than the potential of OH[•]/H₂O (+2.68 eV vs. NHE), which confirm that the photo-generated holes are not capable to oxidize water to yield hydroxyl (OH[•]) radicals in Bi₂MoO₆. The conduction band potential of Bi₂MoO₆ was estimated to be (-0.28 eV vs. NHE), which is more negative than E(O₂/O₂^{•-}) (-0.04 eV vs. NHE) (Li et al., 2018), so it can quickly reduce O₂ to produce superoxide radical O₂^{•-}.

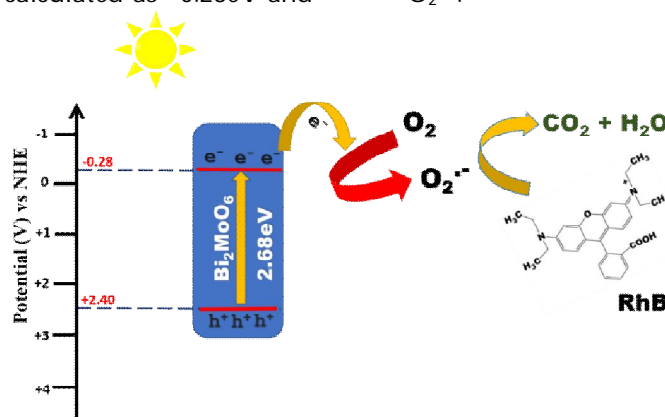


Figure 7: The proposed photocatalytic mechanism over Bi₂MoO₆ under sunlight irradiation

CONCLUSIONS

A simple hydrothermal synthetic route has synthesized the Bi₂MoO₆ photocatalyst. The Bi₂MoO₆ photocatalyst shows excellent photocatalytic performance towards the degradation of 90 % of rhodamine B (RhB) under sunlight irradiation. The corresponding kinetic rate constant of the Bi₂MoO₆ photocatalyst was 0.038 min⁻¹. Bi₂MoO₆ is an effective visible light photocatalyst option for removing various organic dyes in aqueous media due to its strong photocatalytic activity.

REFERENCES

1. Akbari, M. Z., Xu, Y., Lu, Z., & Peng, L. (2021). Review of antibiotics treatment by advance oxidation processes. *Environmental Advances*, 5, 100111. <https://doi.org/10.1016/j.envadv.2021.100111>
2. Calvete, M. J. F., Piccirillo, G., Vinagreiro, C. S., & Pereira, M. M. (2019). Hybrid materials for heterogeneous photocatalytic degradation of antibiotics. *Coordination Chemistry Reviews*, 395, 63–85. <https://doi.org/10.1016/j.ccr.2019.05.004>
3. Dinh, Q. T., Moreau-Guigon, E., Labadie, P., Alliot, F., Teil, M. J., Blanchard, M., & Chevreuil, M. (2017). Occurrence of antibiotics in rural catchments. *Chemosphere*, 168, 483–490. <https://doi.org/10.1016/j.chemosphere.2016.10.106>
4. Durán-Álvarez, J. C., Avella, E., Ramírez-Zamora, R. M., & Zanella, R. (2016). Photocatalytic degradation of ciprofloxacin using mono- (Au, Ag and Cu) and bi- (Au-Ag and Au-Cu) metallic nanoparticles supported on TiO₂ under UV-C and simulated sunlight. *Catalysis Today*, 266, 175–187. <https://doi.org/10.1016/j.cattod.2015.07.033>
5. Homem, V., & Santos, L. (2011). Degradation and removal methods of antibiotics from aqueous matrices - A review. *Journal of Environmental Management*, 92(10), 2304–2347.

- <https://doi.org/10.1016/j.jenvman.2011.05.023>
6. Kortüm, G. (1969). *Reflectance Spectroscopy*, translated by JE Lohr. Springer Verlag, New York.
 7. Li, C., Yu, S., Dong, H., Liu, C., Wu, H., Che, H., & Chen, G. (2018). Z-scheme mesoporous photocatalyst constructed by modification of Sn3O4 nanoclusters on g-C3N4 nanosheets with improved photocatalytic performance and mechanism insight. *Applied Catalysis B: Environmental*, 238(July), 284–293. <https://doi.org/10.1016/j.apcatb.2018.07.049>
 8. Michael, I., Rizzo, L., Mc Ardell, C. S., Manaia, C. M., Merlin, C., Schwartz, T., Dagot, C., & Fatta-Kassinos, D. (2013). Urban wastewater treatment plants as hotspots for the release of antibiotics in the environment: A review. *Water Research*, 47(3), 957–995. <https://doi.org/10.1016/j.watres.2012.11.027>
 9. Qin, K., Zhao, Q., Yu, H., Xia, X., Li, J., He, S., Wei, L., & An, T. (2021). A review of bismuth-based photocatalysts for antibiotic degradation: Insight into the photocatalytic degradation performance, pathways and relevant mechanisms. *Environmental Research*, 199(March), 111360. <https://doi.org/10.1016/j.envres.2021.111360>
 10. Rivera-Utrilla, J., Sánchez-Polo, M., Ferro-García, M. Á., Prados-Joya, G., & Ocampo-Pérez, R. (2013). Pharmaceuticals as emerging contaminants and their removal from water. A review. *Chemosphere*, 93(7), 1268–1287. <https://doi.org/10.1016/j.chemosphere.2013.07.059>
 11. Tauc, J., Grigorovici, R., & Vancu, A. (1966). Optical Properties and Electronic Structure of Amorphous Germanium. *Physica Status Solidi (B)*, 15(2), 627–637. <https://doi.org/https://doi.org/10.1002/pssb.19660150224>
-